



**Queensland University of Technology**  
Brisbane Australia

This is the author's version of a work that was submitted/accepted for publication in the following source:

Zhang, Xingguang, Ke, Xuebin, Zheng, Zhanfeng, Liu, Hongwei, & Zhu, Huaiyong (2014) TiO<sub>2</sub> nanofibers of different crystal phases for transesterification of alcohols with dimethyl carbonate. *Applied Catalysis B : Environmental*, 150-151, pp. 330-337.

This file was downloaded from: <http://eprints.qut.edu.au/66099/>

© © 2013 Elsevier B.V. All rights reserved.

NOTICE: this is the author's version of a work that was accepted for publication in *Applied Catalysis B : Environmental*. Changes resulting from the publishing process, such as peer review, editing, corrections, structural formatting, and other quality control mechanisms may not be reflected in this document. Changes may have been made to this work since it was submitted for publication. A definitive version was subsequently published in *Applied Catalysis B : Environmental*, [150-151, ISSUE#, (5 May 2014)] <http://dx.doi.org/10.1016/j.apcatb.2013.12.035>

**Notice:** *Changes introduced as a result of publishing processes such as copy-editing and formatting may not be reflected in this document. For a definitive version of this work, please refer to the published source:*

<http://dx.doi.org/10.1016/j.apcatb.2013.12.035>

# TiO<sub>2</sub> nanofibers of different crystal phases for transesterification of alcohols with dimethyl carbonate

*Xingguang Zhang, Xuebin Ke,\* Zhanfeng Zheng, Hongwei Liu, and Huaiyong Zhu\**

School of Chemistry, Physics, and Mechanical Engineering, Queensland University of Technology, GPO Box 2434, Brisbane, Qld 4001 (Australia). Fax: (+61) 07 31381804, E-mail: x.ke@qut.edu.au; hy.zhu@qut.edu.au.

**Keywords.** TiO<sub>2</sub> nanofibers, transesterification, apparent activation energy, isotope labeling

**Abstract.** TiO<sub>2</sub> nanofibers with different crystal phases have been discovered to be efficient catalysts for the transesterification of alcohols with dimethyl carbonate to produce corresponding methyl carbonates. Advantages of this catalytic system include excellent selectivity (>99%), general suitability to alcohols, reusability and ease of preparation and separation of fibrous catalysts. Activities of TiO<sub>2</sub> catalysts were found to correlate with their crystal phases which results in different absorption abilities and activation energies on the catalyst surfaces. The kinetic isotope effect (KIE) investigation identified the rate-determining step, and the isotope labeling of oxygen-18 of benzyl alcohol clearly demonstrated the reaction pathway. Finally, the transesterification mechanism of alcohols with dimethyl carbonate catalyzed by TiO<sub>2</sub> nanofibers was proposed, in which the alcohol released the proton to form benzyl alcoholic anion, and subsequently the anion attacks the carbonyl carbon of dimethyl carbonate to produce the target product of benzyl methyl carbonate.

## 1. Introduction

Methylation, carbonylation, carboxylation, and transesterification are important organic reactions and are extensively applied in industry for producing fine chemicals. Conventional processes, for instance, the conversion of alcohols to methyl ethers or methyl carbonates,<sup>1, 2</sup>

heavily depend on the classical base-promoted processes that involve toxic, hazardous, or corrosive compounds, such as alkyl halides, dimethylsulfate and phosgene, and consume over-stoichiometric amounts of strong bases.<sup>3,4</sup> Though efficient, these processes have raised severe concerns on safety and environments.

To address these problems, heterogeneous catalysts have been developed. For example, NaX,<sup>5</sup> NaY,<sup>6</sup> K<sub>2</sub>CO<sub>3</sub><sup>7</sup> and Al<sub>2</sub>O<sub>3</sub><sup>8</sup> are studied, using dialkylcarbonates (ROC(=O)OR), especially the environment-benign reagent of dimethyl carbonate (DMC), as innovative alkylation agents in recent years.<sup>1-4</sup> DMC is a nontoxic and safe compound and shows unprecedentedly high selectivity (>99%) in the mono-methylation or carboxylation of aromatic alcohols, mercaptophenols, mercaptobenzoic acids, oximes, and amines.<sup>1,9</sup> However, more work needs to be done to explore new heterogeneous catalytic materials and to investigate the catalytic mechanism that is still ambiguous in terms of the rate-determining step and the cleavage of chemical bonds of reactants.

The carboxymethylation of bisphenol A with DMC catalyzed by TiO<sub>2</sub>/SBA-15 has been reported.<sup>10</sup> It is stated that the species of Si-O-Ti bonds are active sites and that the interaction mode between Si-O-Ti and DMC plays a critical role in determining the selectivity. This work inspires us to explore whether TiO<sub>2</sub> can catalyze the transesterification of alcohols with dimethyl carbonate, considering the recent discoveries that metal oxides can interact with alcohols to form surface complexes and contribute to efficient catalysis.<sup>11-13</sup> The TiO<sub>2</sub> surface structures have been widely studied as photocatalysts,<sup>14, 15</sup> demonstrating that different crystal phases have different photocatalytic consequences.<sup>16</sup> Primarily, TiO<sub>2</sub> exists in nature in four polymorphs: anatase (tetragonal, space group *I4<sub>1</sub>/amd*), rutile (tetragonal, space group *P4<sub>2</sub>/mnm*), brookite (orthorhombic, space group *Pbca*), and TiO<sub>2</sub>(B) (monoclinic, space group *C<sub>2</sub>/m*)<sup>17, 18</sup>. If TiO<sub>2</sub>

nanofibers can catalyze the transesterification, different crystal phases should exhibit different activities or selectivity, and thus the activation energies on each phase should vary. However these issues have not been clarified in reported studies.

In this study, TiO<sub>2</sub> nanofibers were employed to catalyze the transesterification of alcohols with DMC, and generally it is easier to separate fibrous materials from a liquid reaction system<sup>19</sup>,<sup>20</sup>, compared with nanoparticles. The catalysts were anatase (A), TiO<sub>2</sub>(B), rutile (R), mixed anatase and TiO<sub>2</sub>(B) – TiO<sub>2</sub>(A+B), mixed anatase and rutile – TiO<sub>2</sub>(A+R), commercial anatase and P<sub>25</sub> particles (for control experiments). The scope of alcohols encompassed aromatic alcohols and alkyl alcohols, which indicated that TiO<sub>2</sub> catalysts possessed a general suitability to alcohols in the transesterification. Significantly, high activity and selectivity were achieved. The distribution of products was influenced by the phase compositions, and the catalytic activities also substantially depended on crystal phases of TiO<sub>2</sub> catalysts owing to their different abilities to adsorb reactants and different activation energies required to initiate the reactions. The activation energies of the transesterification on TiO<sub>2</sub>(A), TiO<sub>2</sub>(B), and TiO<sub>2</sub>(R) were obtained by the kinetic study, and the rate-determining step was identified by the kinetic isotope effect (KIE) investigation. These findings, particularly the high selectivity on TiO<sub>2</sub>(B), are promising because the methylcarbonate-ended chemicals are very active reagents for producing high molecular weight polymers, such as polycarbonates in the post-polycondensation step.<sup>21</sup>

## **2. Experimental**

### *2.1 Preparation of catalysts*

All chemicals and commercial anatase and P<sub>25</sub> were purchased from Sigma-Aldrich and were used without further treatment. Hydrogen-form titanate nanofibers (H<sub>2</sub>Ti<sub>3</sub>O<sub>7</sub>) were prepared according to Ref 19. TiO<sub>2</sub> catalysts of different phases were obtained by calcining H<sub>2</sub>Ti<sub>3</sub>O<sub>7</sub> at

different temperatures for 3 h with the step of increasing temperature of 5°C/min: TiO<sub>2</sub>(B) (450°C, B phase of TiO<sub>2</sub>), TiO<sub>2</sub>(A+B) (550°C, uniform mixture of TiO<sub>2</sub>(A) and TiO<sub>2</sub>(B) in one nanofiber, not a mechanical mixture), TiO<sub>2</sub>(A) (700°C, anatase), TiO<sub>2</sub>(A+R) (850°C, uniform mixture of TiO<sub>2</sub>(A) and TiO<sub>2</sub>(R)), TiO<sub>2</sub>(R) (950°C, rutile). After treatment, all materials maintained nanofibrous morphology (*see SEM images in Supplementary data, Section 1*).

## 2.2 Characterizations

X-ray diffraction (XRD) patterns of the samples were recorded on a Philips PANalytical X'Pert PRO diffractometer using CuK $\alpha$  radiation ( $\lambda=1.5418 \text{ \AA}$ ) operating at 40 kV and 40 mA with a fixed slit. The transmission electron microscopy (TEM) study on TiO<sub>2</sub> nanofibers was performed on the instrument of Philips CM200 TEM with the accelerating voltage being 200 kV, and high-resolution TEM (HR-TEM) study was carried out on a FEI Tecnai F20 operating at 200 kV. Diffuse reflectance UV/Visible (DR-UV/Vis) spectra were recorded on a Cary 5000 UV/Vis-Nir Spectrophotometer to investigate the light absorption and emission behaviour of the samples. The measurement of IES (Infrared Emission Spectroscopy) was conducted on a Digilab FTS-60A spectrometer equipped with a TGS detector, and the instrument was modified by replacing the IR source with an emission cell. Identical amounts (in volume) of samples of TiO<sub>2</sub> with different crystal phases were loaded on the sample holder to form a uniform thin layer. During the measurement, the specimen was heated from 100°C to 450°C with the interval being 50°C in the flow of N<sub>2</sub> (15 cm<sup>3</sup>/min controlled by a flow meter) in a closed but not sealed chamber for removing desorbed species from the sample. The interval between the two scans, for instance, between 100°C and 150°C, was two minutes for the sample to stabilize and reach temperature equilibrium. When the specimen was heated, the species adsorbed on the TiO<sub>2</sub> surface, such as adsorbed water and benzyl alcohol, were gradually removed. The extent of the

removal depended on the adsorption strength of the species on the TiO<sub>2</sub> surface. The maximum temperature was 450°C to prevent the specimen from undergoing a phase change. By comparing the loss of adsorbed surface organic species during heating process, the absorption ability of TiO<sub>2</sub> surfaces could be determined because the TiO<sub>2</sub> samples that had weaker adsorption ability lost adsorbed surface complexes more easily. The IES spectra at a lower temperature had more noise owing to the low signal-to-noise ratio resulted from the difference between the sample and the detector.

### *2.3 Catalytic test*

Typically, 0.1 g of TiO<sub>2</sub> catalysts were added into 30 mL DMC and 2.0 mmol benzyl alcohol in a two-necked 100 mL round-bottomed glass flask. The air in the flask was replaced with argon prior to reaction. Then the side mouth of the glass reactor from which samples were taken was sealed by a stopper and the main mouth was connected to a reflux. The reactor was kept at 100 °C in an oil bath with a magnetic stirring bar. The specimens were collected after 8 h, and analyzed in a Gas Chromatography (HP6890 Prometheus, the HP-5 column) to measure the concentration change of benzyl alcohol and products. GC-MS (6890-5793 Pegasus, the HP-5 column) was also employed to determine and analyze the products. Quantification of the products was obtained from the peak area ratios of the reactant and corresponding products. The reaction rate was defined as follows: reaction rate = (moles of reagent converted) / (moles of total active sites × reaction time).

### *2.4 Isotope labeling experiment*

Oxygen-18 (<sup>18</sup>O) isotope-labelled benzyl alcohol (PhCH<sub>2</sub><sup>18</sup>OH) was prepared by following the Ref 22: 0.4 g sodium (Na) metal was added to 3.0 mL 98% H<sub>2</sub><sup>18</sup>O (from Huayì Isotope Co.) in a 25-mL round-bottomed flask, and 2.0 mL benzyl chloride was added into the flask. Then the

mixture was heated by an oil bath to 150°C and refluxed for 48 h with continuous stirring. The products were purified by distillation and the obtained PhCH<sub>2</sub><sup>18</sup>OH was used in the transesterification reaction with DMC on TiO<sub>2</sub>(B) to investigate the kinetic isotope effect (KIE). In addition, the reaction between PhCH<sub>2</sub><sup>18</sup>OH with DMC was conducted in the same procedure as described above just by replacing normal benzyl alcohol with PhCH<sub>2</sub><sup>18</sup>OH. The products were also detected and analyzed by GC and GC-MS.

### 3. Results and Discussions

#### 3.1. Catalytic performance

The conversion of benzyl alcohol was in this order: TiO<sub>2</sub>(B) > TiO<sub>2</sub>(A+B) > TiO<sub>2</sub>(A) > anatase > P<sub>25</sub> > TiO<sub>2</sub>(A+R) > TiO<sub>2</sub>(R), as shown in Table 1. Anatase and P<sub>25</sub> were tested in control experiments, anatase showed a lower conversion than that of TiO<sub>2</sub>(A), and P<sub>25</sub> exhibited slightly higher activity than TiO<sub>2</sub>(A+R) but poor selectivity. The conversion and selectivity were excellent at 100°C on TiO<sub>2</sub>(B) and TiO<sub>2</sub>(A+B), indicating that the product was predominantly benzyl methyl carbonate (BMC). The distribution of products was also influenced by the phase composition, generally, BMC was the dominant product on most catalysts, whereas dibenzyl ether (DBE) was the major product on TiO<sub>2</sub>(R) and TiO<sub>2</sub>(A+R).

Table 2 showed the catalytic performance of TiO<sub>2</sub>(B), which exhibited the best catalytic performance as shown in Table 1, for the transesterification of DMC with several sorts of alcohols to test its general applicability. The range of alcohols covers aromatic alcohols and alkyl alcohols, and most of alcohols reacted with DMC to give the corresponding methyl carbonates with a high activity and excellent selectivity. The conversions could be improved significantly if temperature is raised to 160°C (*see Table S1 in Supplementary data, Section 2*). These results

demonstrated that TiO<sub>2</sub> catalysts had universal applicability for the transesterification of alcohols with DMC.

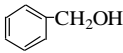
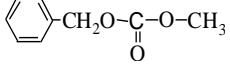
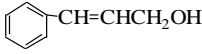
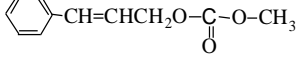
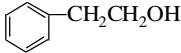
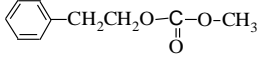
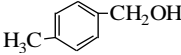
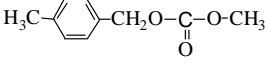
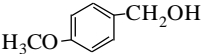
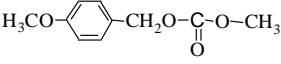
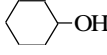
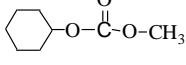
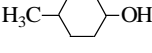
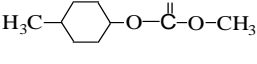
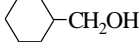
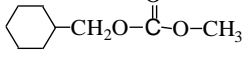
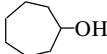
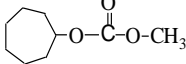
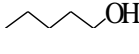
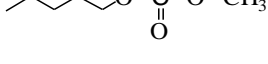
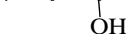
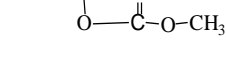
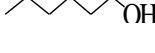
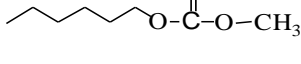
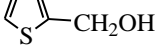
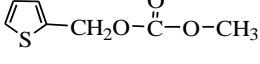
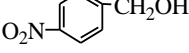
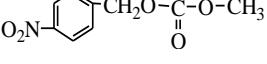
**Table 1.** The conversion and selectivity on different catalysts

Catalyst	Conv. <sup>b</sup>	Reaction Rate [10 <sup>-3</sup> molg <sup>-1</sup> h <sup>-1</sup> ]	Sele. <sup>c</sup> (%)			
	(%)		BME	BMC	DBE	DBC
TiO <sub>2</sub> (A)	24.2	4.83		94.9	5.1	
TiO <sub>2</sub> (B)	39.8	7.94		>99		
TiO <sub>2</sub> (A+B)	37.8	7.54	6.3	93.7		
TiO <sub>2</sub> (R)	6.7	1.34			>99	
TiO <sub>2</sub> (A+R)	9.4	1.88			90.3	9.7
Anatase	20.6	4.12	3.2	90.6	6.2	
P <sub>25</sub>	10.7	2.14	1.9	14.4	76.5	7.2

<sup>a</sup>Reaction temperature. <sup>b</sup>Conversion of benzyl alcohol. <sup>c</sup>BME represents benzyl methyl ether; BMC, benzyl methyl carbonate, DBE dibenzyl ether; and DBC, dibenzyl carbonate. Reaction conditions: DMC (30 mL), benzyl alcohol (2.0 mmol), catalyst (0.1 g), reaction time (8 h), temperature (100 °C), and argon atmosphere.



**Table 2:** Catalytic performances of TiO<sub>2</sub>(B) for several alcohols

Reagent	Preferred product	Conv. <sup>a</sup> (%)	Sele. <sup>b</sup> (%)	Reaction Rate [10 <sup>-3</sup> molg <sup>-1</sup> h <sup>-1</sup> ]
		39.8	>99	7.94
		18.6	47.5	3.71
		40.1	>99	8.01
		48.1	>99	9.61
		70.4	88.3	14.06
		44.9	>99	8.97
		37.9	91.1	7.57
		52.7	>99	10.52
		36.9	>99	7.37
		40.7	>99	8.12
		32.8	>99	6.55
		45.5	>99	9.09
		50.7	>99	10.13
		52.0	>99	10.39

<sup>a</sup>Conversion of the reactant. <sup>b</sup>Selectivity towards the preferred product. Reaction conditions: DMC (30 mL), benzyl alcohol (2.0 mmol), catalyst (0.1 g), reaction time (8 h), temperature (100°C), and argon atmosphere.

### 3.2. XRD and TEM analyzes TiO<sub>2</sub> catalysts

Figure 1 (a) and (b) display the XRD patterns of TiO<sub>2</sub> catalysts. The single-phase nanofiber of TiO<sub>2</sub>(A), TiO<sub>2</sub>(B), and TiO<sub>2</sub>(R) all showed its characteristic diffraction peaks. Both TiO<sub>2</sub>(A+B) and TiO<sub>2</sub>(A+R) indicated a mixed phase structure. The molar ratio between TiO<sub>2</sub>(B) and TiO<sub>2</sub>(A) phase in TiO<sub>2</sub>(A+B) was estimated from the intensity ratio ( $I_{33.4}/I_{37.8}=65.3\%$ ) of the peak at  $2\theta = 33.4^\circ$  to the peak at  $2\theta = 37.8^\circ$ , which were reflections from the ( $\bar{3}11$ ) plane of TiO<sub>2</sub>(B) (JCPDS 74-1940) and the (004) plane of anatase (JCPDS 21-1272), respectively.<sup>19</sup> Similarly, the molar ratio between TiO<sub>2</sub>(R) and TiO<sub>2</sub>(A) in TiO<sub>2</sub>(A+R) was calculated from the intensity ratio ( $I_{27.5}/I_{25.3}=34.5\%$ ) of the peak at  $27.5^\circ$  to the peak at  $25.3^\circ$ , which were reflections from the (110) plane of TiO<sub>2</sub>(R) and the (101) plane of TiO<sub>2</sub>(A), respectively.

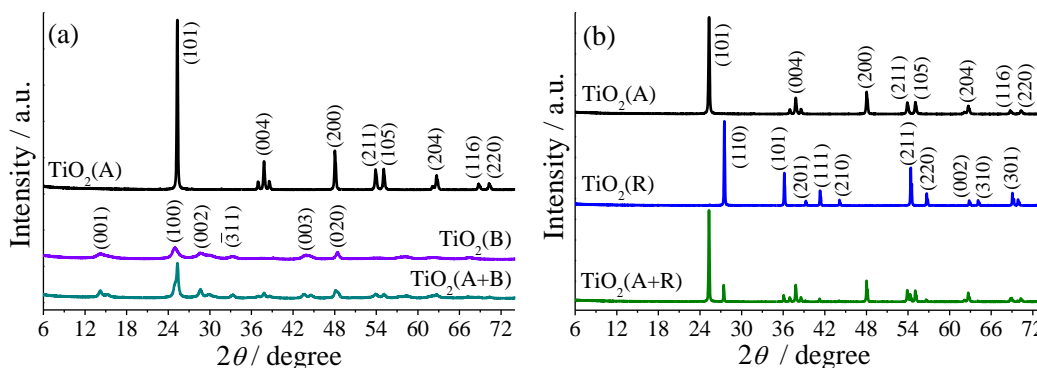


**Figure 1.** (a) X-ray diffraction (XRD) patterns of TiO<sub>2</sub>(A), TiO<sub>2</sub>(B), and TiO<sub>2</sub>(A+B). (b) XRD patterns of TiO<sub>2</sub>(A), TiO<sub>2</sub>(R), and TiO<sub>2</sub>(A+R); (“A” refers to anatase, “B” refers to TiO<sub>2</sub>(B) and “R” refers to rutile).

Detailed crystal phase information of TiO<sub>2</sub>(A), TiO<sub>2</sub>(B), and TiO<sub>2</sub>(A+B) is confirmed by high-resolution TEM analyses as presented in Figure 2 (*and Raman spectra in the Supporting Information, Section 3*). Here we mainly focus on TiO<sub>2</sub>(A) and TiO<sub>2</sub>(B) because they performed much better than TiO<sub>2</sub>(R) did in catalytic activities. The electron diffraction pattern in Figure 2(b) identifies only anatase single crystals; and Figure 2(d) shows the fibers have merely TiO<sub>2</sub>(B) single crystals. Furthermore, the selected area electron diffraction (SAED) analysis confirms the

co-existence of both anatase and  $\text{TiO}_2(\text{B})$  phases in the  $\text{TiO}_2(\text{A+B})$  nanofibers, as shown in Figure 2(e) that the dark anatase grain can be observed on the surface of  $\text{TiO}_2(\text{B})$ . The SAED analyses (Figure 2(g)) show that two phases coexist in a state of intimate contact with each other and join tightly; no voids between the crystals of the two phases are observed. The TEM images and SEM pictures (*Supplementary data, Section 1*) confirm that these samples inherited the fibril morphology of the parent hydrogen-form titanate nanofibers after calcinations.

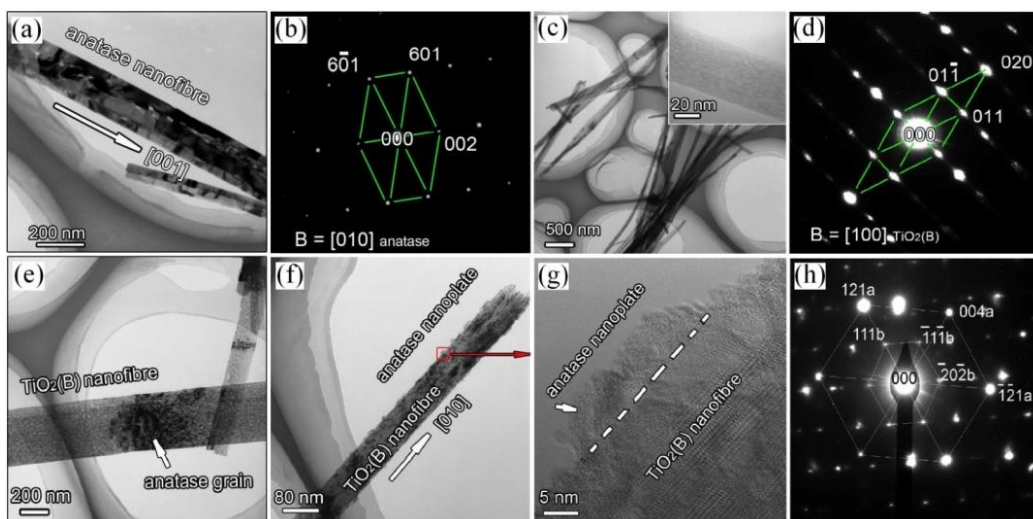


**Figure 2.** High-resolution TEM images of (a)  $\text{TiO}_2(\text{A})$  (anatase) nanofibers, (b) electron diffraction pattern of  $\text{TiO}_2(\text{A})$ , (c)  $\text{TiO}_2(\text{B})$  nanofibers, (d) electron diffraction pattern of  $\text{TiO}_2(\text{B})$ , (e)-(g)  $\text{TiO}_2(\text{A+B})$  nanofibers, and (h) electron diffraction pattern of  $\text{TiO}_2(\text{A+B})$ .

### 3.3. Adsorption ability of $\text{TiO}_2$ catalysts

The ability of  $\text{TiO}_2$  catalysts to adsorb reactants was investigated by UV/Vis spectra and Infrared Emission Spectroscopy (IES). The samples were prepared by mixing 0.1 mL of benzyl alcohol or DMC and 0.1 g of  $\text{TiO}_2$  catalysts together for 4 h at room temperature, followed by washing thoroughly and drying the specimens at  $80^\circ\text{C}$  under vacuum conditions for 24 h. In doing this at the same conditions, the amount of residue adsorbates and the removal extents

under thermal treatment should qualitatively reflect the adsorption ability of  $\text{TiO}_2$  catalysts. The spectrum of pure benzyl alcohol and DMC were also collected for comparison.

The UV/Vis spectra of benzyl alcohol,  $\text{TiO}_2$  catalysts, and benzyl alcohol-adsorbed  $\text{TiO}_2$  catalysts (Figure 3 (a)) showed that benzyl alcohol and  $\text{TiO}_2$  catalysts exhibited no measurable absorption in the visible region (please note that the curves have been vertically moved upward to arrange neatly for clear comparison). As for the benzyl-adsorbed  $\text{TiO}_2$  catalysts,  $\text{TiO}_2(\text{B})$  and  $\text{TiO}_2(\text{A+B})$  exhibited obvious absorption of visible light,  $\text{TiO}_2(\text{A})$  showed slight absorption; whereas  $\text{TiO}_2(\text{A+R})$  and  $\text{TiO}_2(\text{R})$  almost had no absorption. These results demonstrated that  $\text{TiO}_2(\text{B})$  and  $\text{TiO}_2(\text{A+B})$  had stronger ability to adsorb benzyl alcohol than  $\text{TiO}_2(\text{A+R})$  and  $\text{TiO}_2(\text{R})$  did. In some studies, the interaction between benzyl alcohol and anatase is assigned to the  $\text{TiO}_2$  surfaces interacting with the  $-\text{CH}_2\text{OH}$  group or the phenyl ring of benzyl alcohol.<sup>23, 24</sup>

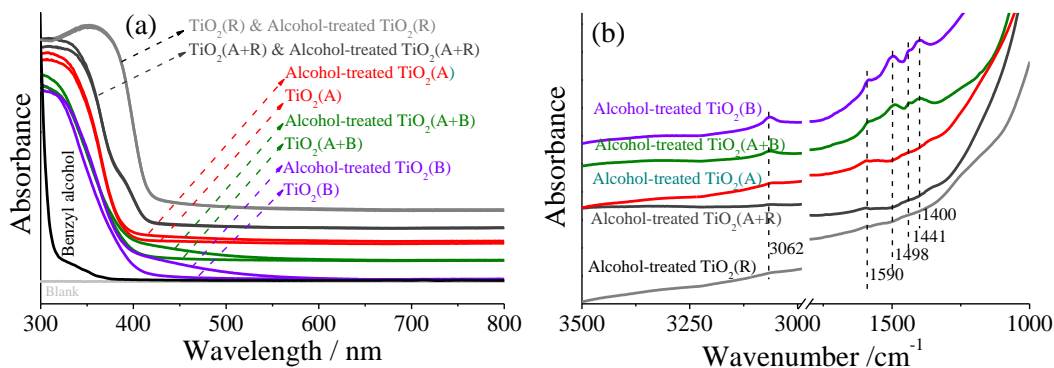


**Figure 3.** (a) UV/Vis spectra of benzyl alcohol,  $\text{TiO}_2$  catalysts and benzyl alcohol-adsorbed  $\text{TiO}_2$  catalysts (the “ $\text{TiO}_2(\text{R})$  & DMC-treated  $\text{TiO}_2(\text{R})$ ” means that two curves of each were so similar that they overlapped); (b) IES spectra of benzyl alcohol-adsorbed  $\text{TiO}_2$  catalysts collected at  $400^\circ\text{C}$ .

To further determine the adsorption ability of  $\text{TiO}_2$  catalysts, the IES spectra (Figure 3(b)) of benzyl alcohol-adsorbed  $\text{TiO}_2$  catalysts were collected at  $400^\circ\text{C}$ . At this temperature, the crystal phase of  $\text{TiO}_2$  catalysts remained unchanged, but partial organic species on the surface of some catalysts had been removed because of different adsorption abilities of  $\text{TiO}_2$  catalysts. To be

clear, the adsorbates may be not benzyl alcohol molecules at 400°C but decomposed organic species, such as aromatic rings, benzyloxy/alkoxy groups that are surface complexes formed between alcohols and metal oxides.<sup>25</sup> Several peaks could be identified from the spectra. The peak centered at 3062 cm<sup>-1</sup> and 1440 cm<sup>-1</sup> were assigned to the C-H stretching vibration and the C-H in-plane bending vibration of the aromatic rings.<sup>24</sup> The band at 1590 cm<sup>-1</sup> indicated the C-C ring stretching vibration.<sup>26</sup> The band at 1498 cm<sup>-1</sup> could be readily ascribed to the skeletal vibration of the aromatic ring and the band centered at 1400 cm<sup>-1</sup> could be identified as the ring stretching mode.<sup>27</sup> From the extent of the removal of decomposed organic species, one can deduce the ability of TiO<sub>2</sub> catalysts to adsorb the organic species, because the interaction between them and TiO<sub>2</sub> catalysts originated from strong chemical adsorption after thoroughly washing and 24-hour drying under the vacuum condition. The weaker adsorption results in losing adsorbed organic species more easily on such as TiO<sub>2</sub>(R) which lost every peak of organic species at 400°C, whereas TiO<sub>2</sub>(B) still held some surface organic species. Therefore, it could be generally concluded that the absorption ability of TiO<sub>2</sub> catalysts was in the following order: TiO<sub>2</sub>(B) > TiO<sub>2</sub>(A+B) > TiO<sub>2</sub>(A) > TiO<sub>2</sub>(A+R) > TiO<sub>2</sub>(R), which corresponded excellently to the tendency as shown in the UV/Vis spectra (Figure 3(a)).

The UV/Vis spectra of DMC, TiO<sub>2</sub> catalysts, and DMC-adsorbed TiO<sub>2</sub> catalysts showed that no obvious difference could be found in the spectra of each TiO<sub>2</sub> catalyst and its DMC-adsorbed counterpart (*see Supplementary data, Section 4*). Moreover, the IR-ATR (Attenuated Total Reflectance) spectra of DMC, TiO<sub>2</sub>(B) and DMC-adsorbed TiO<sub>2</sub>(B) provided no convincing evidence that DMC was still adsorbed on the surface of TiO<sub>2</sub>(B) after washing and 24-hour drying under the vacuum condition. These results suggested that TiO<sub>2</sub> catalysts had extremely weak ability to adsorb DMC molecules.

### 3.4. Kinetic study

The difference in catalytic activities and the adsorption ability of TiO<sub>2</sub> catalysts inspire us that the activation energies on the TiO<sub>2</sub> catalysts should be different. Here TiO<sub>2</sub>(B), TiO<sub>2</sub>(A) and TiO<sub>2</sub>(R) were used to investigate the activation energy of the reaction between benzyl alcohol and DMC at several temperatures: 40°C, 60°C, 80°C and 100°C. Samples were collected after different periods of reaction time within 8 hours to calculate the conversion of benzyl alcohol ( $X_b$ ), and a first-order dependence of the reaction rate on the concentration of benzyl alcohol was found. The plot of  $-\ln(1 - X_b)$  versus the reaction time  $t$  created several straight lines (*see Supplementary data, Section 5*), according to the equation of the first-order reaction:  $-\ln(1 - X_b) = kt$ , in which  $k$  is the rate constant of the reaction. For each line, the slope is equal to the negative value of the rate constant  $k$  so that four values of  $k$  can be obtained at four different temperatures for each catalyst.

According to the Arrhenius equation, three straight lines of  $\ln(k)$  versus  $(1/T)$  can be obtained, corresponding to TiO<sub>2</sub>(B), TiO<sub>2</sub>(A) and TiO<sub>2</sub>(R) as shown in Figure 4, and the value of the slope equals to  $-E_a/R$  ( $E_a$  means the apparent activation energy). Then the activation energies on TiO<sub>2</sub>(B) (denoted as  $E_B$ ), TiO<sub>2</sub>(A) (denoted as  $E_A$ ), and TiO<sub>2</sub>(R) (denoted as  $E_R$ ) can be calculated, being 24.2 kJmol<sup>-1</sup>, 33.0 kJmol<sup>-1</sup> and 58.5 kJmol<sup>-1</sup>, respectively. These results again suggested that TiO<sub>2</sub>(B) could activate the reaction between benzyl alcohol and DMC more easily than TiO<sub>2</sub>(R) does.

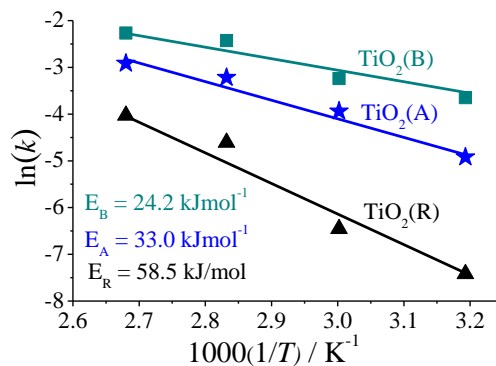


**Figure 4.** The plot of  $\ln(k)$  versus  $(1/T)$  for deriving the apparent activation energy. Reaction conditions: DMC (30 mL), benzyl alcohol (2.0 mmol), catalyst (0.1 g), and argon atmosphere.

### 3.5. Discussion on the difference in activities of $\text{TiO}_2$ catalysts

One may wonder why  $\text{TiO}_2$  catalysts with different crystal structures exhibit different activities. First, the adsorption ability of  $\text{TiO}_2$  catalysts should play a vital role in determining the catalytic activity because stronger adsorption ability facilitates the concentration of reactants from solvent. The UV/Vis and IES spectra of benzyl alcohol-adsorbed  $\text{TiO}_2$  catalysts have demonstrated that the order of adsorption ability matches excellently to the catalytic activities of the  $\text{TiO}_2$  catalysts in the transesterification of benzyl alcohol with DMC. Second, the results of kinetic study suggested that the activation energy on  $\text{TiO}_2(\text{B})$  is much lower than that on  $\text{TiO}_2(\text{R})$ , thus activating reactants more easily to initiate the transesterification. Third, the difference in the surface areas of  $\text{TiO}_2$  catalysts should have a negligible influence on the catalytic activities because the Brunauer-Emmett-Teller (BET) surface areas of these  $\text{TiO}_2$  catalysts in use are similar, ranging from 19.8 to 38.6  $\text{m}^2\text{g}^{-1}$ , (see Table S2 in Supplementary data, Section 6). Therefore, it should be safe to conclude that the difference in catalytic activities of  $\text{TiO}_2$  catalysts results from their different abilities to adsorb and activate reactants.

### 3.6. Investigation of $^{16}\text{O}/^{18}\text{O}$ kinetic isotope effect (KIE) and reaction pathway

The oxygen-18 isotope labeled benzyl alcohol ( $\text{PhCH}_2^{18}\text{OH}$ ) was employed to identify which bond of benzyl alcohol or DMC broke, and whether the breakage of this bond determined the reaction rate (rate-determining step). The experiment was performed on  $\text{TiO}_2(\text{B})$  at  $100^\circ\text{C}$  just as the experiment done for normal benzyl alcohol ( $\text{PhCH}_2\text{OH}$ ). Samples were collected to calculate the conversions ( $X_b$ ), and a linear relationship between  $-\ln(1 - X_b)$  and the reaction time  $t$  was obtained (see Figure 5). The slope of the line corresponds to the rate constant  $k$ : for  $\text{PhCH}_2^{18}\text{OH}$ ,  $k_{18} = 3.79 \times 10^{-6} \text{ s}^{-1}$  and for  $\text{PhCH}_2^{16}\text{OH}$ ,  $k_{16} = 1.89 \times 10^{-5} \text{ s}^{-1}$ . Thus  $\text{KIE} = k_{16}/k_{18} = 4.99$ , indicating that the bond breakage of  $\text{C}-^{18}\text{O}$  or  $^{18}\text{O}-\text{H}$  was the rate-determining step.<sup>22, 28</sup>

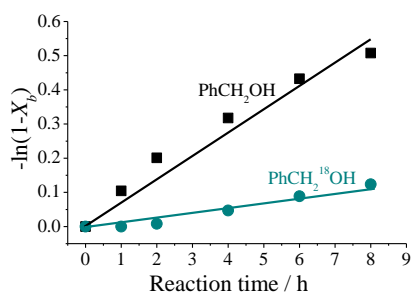
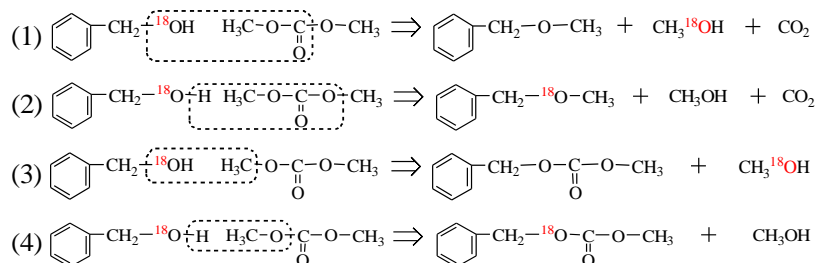


**Figure 5:** Comparison between the transesterification of DMC with benzyl alcohol ( $\text{PhCH}_2\text{OH}$ ) and  $^{18}\text{O}$ -enriched benzyl alcohol ( $\text{PhCH}_2^{18}\text{OH}$ ). The slopes of the lines correspond to the rate constants. Reaction conditions: DMC (30 mL), benzyl alcohol (2.0 mmol), catalyst (0.1 g), and reaction time (8 h), temperature ( $100^\circ\text{C}$ ), and argon atmosphere.

In the reaction between benzyl alcohol and DMC, four major reactions (equations (1) to (4) as shown in Scheme 1) may occur, depending on the positions in which the chemical bonds break:



**Scheme 1:** Four possible reactions between benzyl alcohol and dimethyl carbonate.



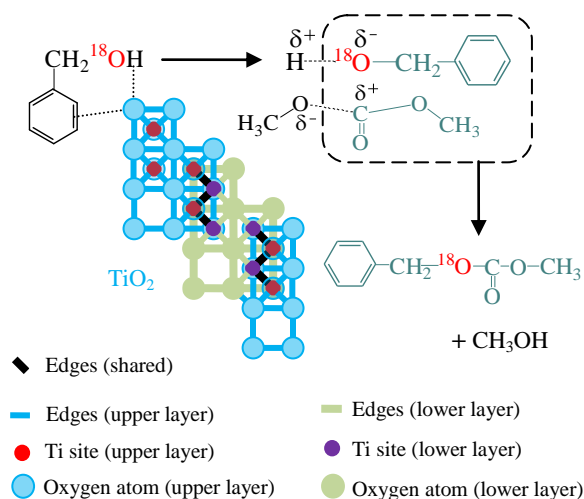
According to the analysis of GC-MS, only the product of  $^{18}\text{O}$ -enriched benzyl methyl carbonate was detected when  $\text{PhCH}_2^{18}\text{OH}$  was used (*see more details in Supplementary data, Section 7*). Therefore, the equation (1), (2) and (3) could be ruled out, and the reaction path was the equation (4). It became transparent that the bond cleavage was on O-H in benzyl alcohol and on  $\text{CH}_3\text{O-C}$  in DMC to produce the desired product of benzyl methyl carbonate.

### 3.7 Mechanistic study

In some studies, DMC conformers are observed on such as NaY and  $\text{TiO}_2/\text{MCM-41}$ ,<sup>6, 29</sup> showing that the electric-field-induced polarization of DMC molecules can lead to the activation (elongation and weakening) of the O- $\text{CH}_3$  and/or C- $\text{OCH}_3$  bonds. The activated DMC molecules can form both *cis-cis* and *cis-trans* species (conformers) to give carboxylated products ( $<90^\circ\text{C}$ ) or methylated products ( $>120^\circ\text{C}$ ).<sup>1</sup> However, the results of the UV/Vis and the IR-ATR spectra (*see Supplementary data, Section 4*) cannot verify a strong interaction between DMC and  $\text{TiO}_2$  catalysts. Therefore, we tentatively speculate that the catalytic activity of  $\text{TiO}_2$  catalysts stems from the direct activation of benzyl alcohol by  $\text{TiO}_2$  catalysts, attended by reaction with DMC in the proximity of activated benzyl alcohol molecules. Moreover, the fact that merely carboxylated products were detected on  $\text{TiO}_2(\text{B})$  at  $160^\circ\text{C}$  indicated that no other DMC conformers formed in the reactions (*see Table S1 Supplementary data, Section 2*).

On the basis of experimental results and relevant literature, a possible mechanism on the transesterification of benzyl alcohol with DMC on  $\text{TiO}_2(\text{B})$  can be proposed as shown in Scheme 2.  $\text{TiO}_2(\text{B})$  adsorbed benzyl alcohol molecules on the surfaces through the interaction with the  $-\text{CH}_2\text{OH}$  group or the phenyl rings.<sup>23, 24</sup> Then the adsorbed benzyl alcohol molecules were activated by  $\text{TiO}_2(\text{B})$  and reacted with DMC. As demonstrated by the isotope labeling

experiment that benzyl alcohol released its proton ( $H^+$ ) from the hydroxyl group (rate-determining step) to produce the benzyl alcoholic anion ( $PhCH_2O^-$ ), which attacked the carbonyl carbon of DMC to give the product of BMC. The released proton ( $H^+$ ) reacted with the methoxy anion ( $CH_3O^-$ ) to give methanol.



**Scheme 2.** Proposed mechanism on the transesterification of benzyl alcohol with dimethyl carbonate on  $TiO_2(B)$ . The illustration of the structure of  $TiO_2(B)$  projected along the  $[010]$  direction.<sup>30</sup>

#### 4. Conclusion

The transesterification of alcohols with dimethyl carbonate was discovered to successfully proceed on  $TiO_2$  nanofibrous catalysts with different crystal phases. Several basic conclusions could be obtained on the grounds of experimental results.

Catalytic activities at  $100^\circ C$  were:  $TiO_2(B) > TiO_2(A+B) > TiO_2(A) > anatase > P_{25} > TiO_2(A+R) > TiO_2(R)$ , and the selectivity on most catalysts was excellent ( $>99\%$ ). The difference in catalytic activities was demonstrated to correlate with the adsorption ability and the different activation energies on  $TiO_2$  catalysts.

The KIE investigation and the mechanistic study by  $^{18}O$  isotope labeling of benzyl alcohol substantially identified the rate-determining step and the reaction pathway, in which the O-H

bond of benzyl alcohol cleaved to give the proton ( $H^+$ ) and the benzyl alcoholic anion ( $PhCH_2O^-$ ) that attacked the carbonyl carbon of DMC to produce the desired product of benzyl methyl carbonate.

Finally, the  $TiO_2$ -catalyzed transesterification mechanism was proposed, and the mechanism was partly different from that occurs on zeolite or acid-base catalysts, because  $TiO_2$  catalysts produced no methylated products even though the reaction temperature was higher than  $120^\circ C$ . Moreover,  $TiO_2$  catalysts can also be repeatedly used while maintaining excellent catalytic activity (*see Supplementary data, Section 8*), and most significantly, we discover that  $TiO_2$ -based catalysts offer a great promise in thermal-driven reactions instead of exclusively in photocatalytic reactions.

### **Acknowledgement**

This research is supported by the Australian Research Council (ARC) and X. Ke is indebted to QUT and the Queensland State Government for a Smart Futures Fellowship.

### **Appendix: Supplementary data**

Supplementary data associated with this article can be found in the online version, including Raman spectra of  $TiO_2$  nanofibers of different crystal phases, SEM images of different phases of  $TiO_2$  catalysts, UV/Vis and IR spectra of DMC and  $TiO_2$ , BET surface areas of  $TiO_2$  catalysts, Kinetic study, plots of  $-\ln(1-X_b)$  versus the reaction time, results of oxygen-18 labeled benzyl alcohol ( $PhCH_2^{18}OH$ ), reusability of  $TiO_2(A)$  and  $TiO_2(B)$ , the catalytic performance of  $TiO_2(B)$  for several alcohols at  $160^\circ C$ .

### **References**

[1] P. Tundo, M. Selva, *Acc. Chem Res.* 35 (2002) 706-716.

- [2] B. Xu, R. J. Madix, C.M. Friend, *J. Am. Chem. Soc.* 133 (2011) 20378-20383.
- [3] A.-A. G. Shaik, S. Sivaram, *Chem. Rev.* 96 (1996) 951-976.
- [4] P. Anastas, N. Eghbali, *Chem. Soc. Rev.* 39 (2010) 301-312.
- [5] M. Selva, E. Militello, M. Fabris, *Green Chem.* 10 (2008) 73-79.
- [6] F. Bonino, A. Damin, S. Bordiga, M. Selva, P. Tundo, A. Zecchina, *Angew. Chem. Int. Ed.* 117 (2005) 4852-4855.
- [7] M.M. Fan, P.B. Zhang, *Energy Fuels* 21 (2007) 633-635.
- [8] R.X. Bai, Y. Wang, S. Wang, F.M. Mei, T. Li, G.X. Li, *Fuel Process Technol.* 106 (2013) 209-214.
- [9] Z.-H. Fu, Y. Ono, *J. Catal.* 145 (1994) 166-170.
- [10] K. M. Su, Z.H. Li, B.W. Cheng, K. Liao, D.X. Shen, Y.F. Wang, *J. Mol. Catal. A* 315 (2010) 60-68.
- [11] H. Kominami, A. Tanaka, K. Hashimoto, *Chem. Commun.* 46 (2010) 1287-1289.
- [12] A. Tanaka, K. Hashimoto, H. Kominami, *Chem. Commun.* 47 (2011) 10446-10448.
- [13] S. Sarina, H.Y. Zhu, Z.F. Zheng, S. Bottle, J. Chang, X.B. Ke, J.-C. Zhao, Y.N. Huang, A. Sutrisno, M. Willans, G.R. Li, *Chem. Sci.* 3 (2012) 2138-2146.
- [14] P.R. Liu, H.M. Zhang, H.G. Liu, Y. Wang, X.D. Yao, G.S. Zhu, S.Q. Zhang, H.J. Zhao, *J. Am. Chem. Soc.* 133 (2011) 19032-19035.
- [15] H.W. Liu, D.J. Yang, Z.F. Zheng, X.B. Ke, E. Waclawik, H.Y. Zhu, R.L. Frost, *J. Raman Spectrosc.* 41 (2010) 1331-1337.
- [16] Z.F. Zheng, J. Teo, X. Chen, H.W. Liu, Y.Yuan, E.R. Waclawik, Z.Y. Zhong, H.Y. Zhu, *Chem. Eur. J.* 16, (2010) 1202-1211.
- [17] L.J. Liu, J. Chan, T.K. Sham, *J. Phys. Chem. C* 114 (2010) 21353-21359.

- [18] R.L. Penn, J.F. Banfield, *Am. Mineral.* 84 (1999) 871-876.
- [19] D.J. Yang, H.W. Liu, Z.F. Zheng, Y. Yuan, J.C. Zhao, E.R. Waclawik, X.B. Ke, H.Y. Zhu, *J. Am. Chem. Soc.* 131 (2009) 17885-17893.
- [20] H.Y. Zhu, Y. Lan, X.P. Gao, S.P. Ringer, Z.F. Zheng, D.Y. Song, J.C. Zhao, *J. Am. Chem. Soc.* 127, (2005) 6730-6736.
- [21] O. Haba, I. Itakura, M. Ueda, S. Kuze, *J. Polym. Sci. Part A: Polym. Chem.* 37 (1999) 2087-2093.
- [22] M. Zhang, Q. Wang, C.C. Chen, L. Zang, W.H. Ma, J.C. Zhao, *Angew. Chem. Int. Ed.* 68 (2009) 6081-6084.
- [23] S. Higashimoto, N. Kitao, N. Yoshida, T. Sakura, M. Azuma, H. Ohue, Y. Sakata, *J. Catal.* 266, (2009) 279-285.
- [24] S. Kim, W. Choi, *J. Phys. Chem. B* 109, (2005) 5143-5149.
- [25] M.J. Hu, J.J. Xu, J.F. Gao, S.L. Yang, J.S.P. Wong, R.K.Y. Li, *Dalton Trans.* 42 (2013) 9777-9784.
- [26] X.H. Guan, G.H. Chen, C. Shang, *J. Environ. Sci.* 19 (2007) 438-443.
- [27] F. Ungureanu, L. Voicu, I. Andrei, *J. Optoelectron. Adv. Mater.* 8, (2006) 315-318.
- [28] H. Bohets, B. J. van der Veken, *Phys. Chem. Chem. Phys.* 1 (1999) 1817-1826.
- [29] F. Wang, W. Ueda, J. Xu, *Angew. Chem. Int. Ed.* 124 (2012) 3949 -3953.
- [30] T. Hongo, A. Yamazaki, *Micropor. Mesopor. Mater.* 142 (2011) 316-321.